

ENGINEERING EVALUATION OF POST-LIQUEFACTION RESIDUAL STRENGTHS

by

Raymond B. Seed
University of California at Berkeley

The past decade has seen rapid advances in the understanding of post-liquefaction residual strength (and associated stress-deformation behavior). Despite this progress, the intrinsic difficulties involved continue to render the engineering assessment and use of post-liquefaction residual “undrained” strengths ($S_{u,r}$) both difficult and somewhat prone to controversy. These very brief notes will discuss key issues, provide illustrations of key principles and phenomena, and will conclude with succinct recommendations for current practice.

At the heart of the issue is the “critical state” concept, illustrated schematically in Figure 1. Soils at an initial “state” (void ratio and effective confining stress) are either “loose” or “dense” depending upon whether they are above or below a curved boundary called the critical state line (CSL). “Dense” soils (initially below the CSL) will seek to dilate when sheared, and “loose” soils (initially above the CSL) will seek to contract or densify when sheared. When sheared under fully drained conditions, soils will contract or dilate until their “state” (σ' and e) reaches the CSL, after which further shearing causes no further change in volume (or void ratio, e). When sheared under undrained conditions, contractive (“loose”) soils move towards the CSL by decreasing their effective stress (σ') by means of increasing pore pressures (Δu). Similarly, dilatent soils seek to move laterally to the CSL by increasing σ' (by pore pressure decrease, $-\Delta u$).

It would thus appear that all one needs to do is: (a) define the CSL for a given soil, (b) evaluate the in-situ void ratio (σ_o), and (c) invoke the critical state principle to evaluate the eventual (critical state) residual strength for undrained loading. Unfortunately, it is a bit more complicated than this.

Sample disturbance effects are of course, problematic. Poulos and Castro (Poulos, et al., 1985) proposed a “steady state” methodology to attempt to correct for inevitable sampling disturbance, but their approach proved both unacceptably volatile (sensitive), and also highly unconservative when compared with field case histories. Figure 2 is an excellent example. This figure shows $S_{u,r}$ values developed by the “steady state” methodology for a number of projects compared against a range of back-calculated $S_{u,r}$ values from field failure case histories. The “steady state” method can be seen to be randomly and unconservatively biased.

Over the past decade, three principal reasons for this have emerged. The first is that $S_{u,r}$ varies as a function of initial effective (consolidation) confining stress (σ'_o). Contrary to pure critical state theory, $S_{u,r}$ increases slightly as σ'_o increases (at the same post-consolidation void ratio, e_o). This is illustrated in Figure 3, which shows stress paths for a suite of IC-U triaxial tests of samples consolidated to identical e_o , but different σ'_o . (In this figure, $p = (\sigma'_1 + \sigma'_2 + \sigma'_3)/3$ and $q = \sigma_1 - \sigma_3$.)

A second factor is test type (stress path or shearing strain path). $S_{u,r}$ is much higher in conventional IC-U triaxial compression than in triaxial extension or undrained simple shear. Both simple shear and triaxial extension routinely provide strengths lower than conventional triaxial compression, and by large factors (5 to 10 are common) at the same void ratio, e_o . Figure 3 contrasts stress paths for samples of identical e_o sheared in triaxial compression and extension. Figure 4 presents a plot, for one sand, of $S_{u,r}$ vs. e_o for (a) triaxial compression, (b) triaxial extension, and (c) undrained simple shear. Unfortunately, triaxial extension and simple shear provide the lowest $S_{u,r}$ (for any given soil, either might be a bit lower than the other), and conventional triaxial compression provides very unconservative values. Even more unfortunate is the fact that field engineering cases are generally dominated by simple shear.

A final factor that complicates field evaluation of $S_{u,r}$ is localized void redistribution. In a layered soil (and field soils are layered), within a given sub-layer, conditions may be "globally" undrained during and immediately after seismic loading. There will, however, be local movements of pore fluid (and thus void ratio), even if the overall volume remains constraint. Solid particles tend to settle, and pore fluid to rise. Accordingly, the void ratio at the tops of sub-layers tends to increase slightly. (In very extreme cases a "blister" or thin film of water can form here). Even a slight increase in void ratio results in a significant decrease in $S_{u,r}$. Nature, given a choice, can then exploit this by selectively shearing through the weakened zone. An illustration is shown in Figure 5. In this centrifuge model, a dam was built "backwards" with a saturated sand core and surrounding impervious clay shells. Subjected to shaking, the sand liquefied as a result of localized void redistribution. The surrounding clay prevented escape of water, and the sand volume (and average void ratio) remained constant. The base of the sand densified, however, and the upper sand loosened. The embankment then suffered a sliding failure, shearing along the top of the sand (the loosened zone with lowest $S_{u,r}$).

It is not currently practicable to evaluate field sub-layering in sufficient detail as to support predication of likely local void redistribution. Thus, detailed sampling and testing programs are not currently the recommended approach for in-situ evaluation of $S_{u,r}$. Instead, the use of empirical correlations, based on back-analyses of full-scale field failure case histories are recommended. Back-analyses of failure case histories naturally incorporate void redistribution effects, and are also (correctly) dominated by simple shear deformation.

These back-analyses are also, however, rendered difficult due to momentum effects. Failure masses do not usually come to rest (in liquefaction failures) at F.S. = 1.0. Instead, F.S. \approx 1.1 to 1.4 is more common, as the moving mass acquires momentum, and strength must be used to overcome this momentum and bring the mass to rest. Because these momentum effects are difficult to quantify, back-analyses can be a bit controversial and published opinions for given case histories can vary. It matters a bit who does the evaluation and analyses.

Figure 6 shows back-calculated values of $S_{u,r}$ vs. corrected SPT N-values for a number of failure case histories. The N-values are corrected for overburden effects and energy and equipment effects (to $N_{1,60}$), and are then further corrected for fines content to yield "equivalent clean sand" values ($N_{1,60,cs}$). The clean sand corrections (ΔN) are as follow:

<u>% Fines</u>	<u>ΔN</u>
10%	+1
25%	+2
50%	+4
75%	+5
(>75%)	(+5)

Figure 7 is a similar figure, based on similar back-analyses, but based on the premise that $S_{u,r}/P = \text{constant}$. (That is $= S_{u,r}/\sigma'_o = \text{constant}$.) As observed earlier, $S_{u,r}$ does indeed increase somewhat with increased σ'_o , but not as a linear function of σ'_o . Figure 8 shows the data from Figure 3, along with the resultant values of $S_{u,r}/P$ for this suite of tests. $S_{u,r}/P$ is much higher at low P , and decreases with increased P . This is typical for all soils of interest for seismically-induced liquefaction work.

So what is an engineer to do?

Figure 6 (which neglects the moderate increase of $S_{u,r}$ with increased σ'_o) is based of failure case histories with average or representative values of σ'_o generally in the range of 0.5 to 2 atmospheres (0.5 to 2 kg/cm² or 0.5 to 2.0 tons/ft².) This is the common range of interest for surface deformations and shallow foundations. At greater depths ($\sigma'_o > 2 \text{ atm.}$), these values of $S_{u,r}$ will be somewhat conservative. It is recommended that values in the lower half of the band be used for $0.5 < \sigma'_o < 2.0 \text{ atm.}$, and somewhat higher values can be justified at greater depths.

The values of Figure 7 are also back-calated for cases with representative or average values of σ'_o generally in the range of 0.5 to 2.0 atmospheres, but the variance in Figure 7 is high as $S_{u,r}/P$ varies considerably for any given soil in this light stress range. It would be very unconservative to attempt to extrapolate Figure 7 to greater depths, as $S_{u,r}/P$ would decrease with increased σ'_o .

A common question is: what happens at higher N-values? The curved zones of Figures 6 and 7 will continue to bend upwards as N-values increase. There are, however, two important recommended limits on $S_{u,r}$. The first is potential cavitation. The pore fluid will cavitate at $u = -1 \text{ atm.}$, and no further pore pressure reduction can occur. This puts an absolute limit on the $S_{u,r}$ that can be mobilized, and requires evaluation of u_o in-situ. An even lesser limit on $S_{u,r}$ is also recommended, however, and this takes precedence over the cavitation limit. It is recommended that design values of $S_{u,r}$ not exceed the fully-drained static strength of the soil. The reasoning here includes the observation that little flow of pore fluid, and over very short distances, can be sufficient to satisfy the "dilatent suction" of a confined, dilatent shearing surface or narrowly-banded shear zone.

References

Arulanadan, K., Seed, H.B., Yogachandron, C., Muraleetharan, K. and Seed, R. B. (1993). "Centrifuge Study on Volume Changes and Dynamic Stability of Earth Dams", J. of Geot. Eng., ASCE, Vol. 119, No. 11, pp. 1717-1728.

Harder, L. F. (1988). "Use of Penetration Tests to Determine the Cyclic Loading Resistance of Gravelly Soils During Earthquake Shaking," Ph.D. Thesis, University of California at Berkeley.

Poulos, S., Castro, G., and France, J. (1985). "Liquefaction Evaluation Procedure," J. Geotech. Engrg., ASCE, 111(6), 772-792.

Riemer, M. F. (1992). "The Effects of Testing Conditions on the Constitutive Behavior of Loose, Saturated Sand Under Monotonic Loading." Ph.D. Thesis, University of California at Berkeley.

Seed, R. B., and Harder, L. (1990). "SPT-Based Analysis of Cyclic Pore Pressure Generation and Undrained Residual Strengths." Proc., H. B. Seed Memorial Symp., BiTech, Vancouver, B.C., (2), 351-376.

Stark, T. D., and Mesri, G. (1992). "Undrained Shear Strength of Liquefied Sands for Stability Analysis." J. Geotechn. Engrg. Div., ASCE, 118(11), 1727-1747.

Von Thun, J. Lawrence (1986) "Analysis of Dynamic Compaction Foundation Treatment Requirements, Stage I, Jackson Lake Dam," Technical Memorandum No. TM-JL-230-26, U.S. Bureau of Reclamation.

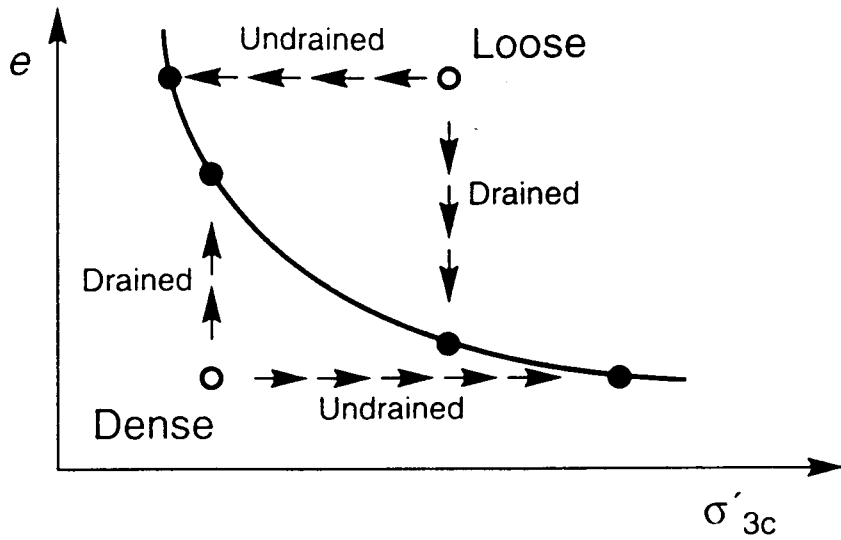


Figure 1: Schematic Illustration of the Critical State Principle

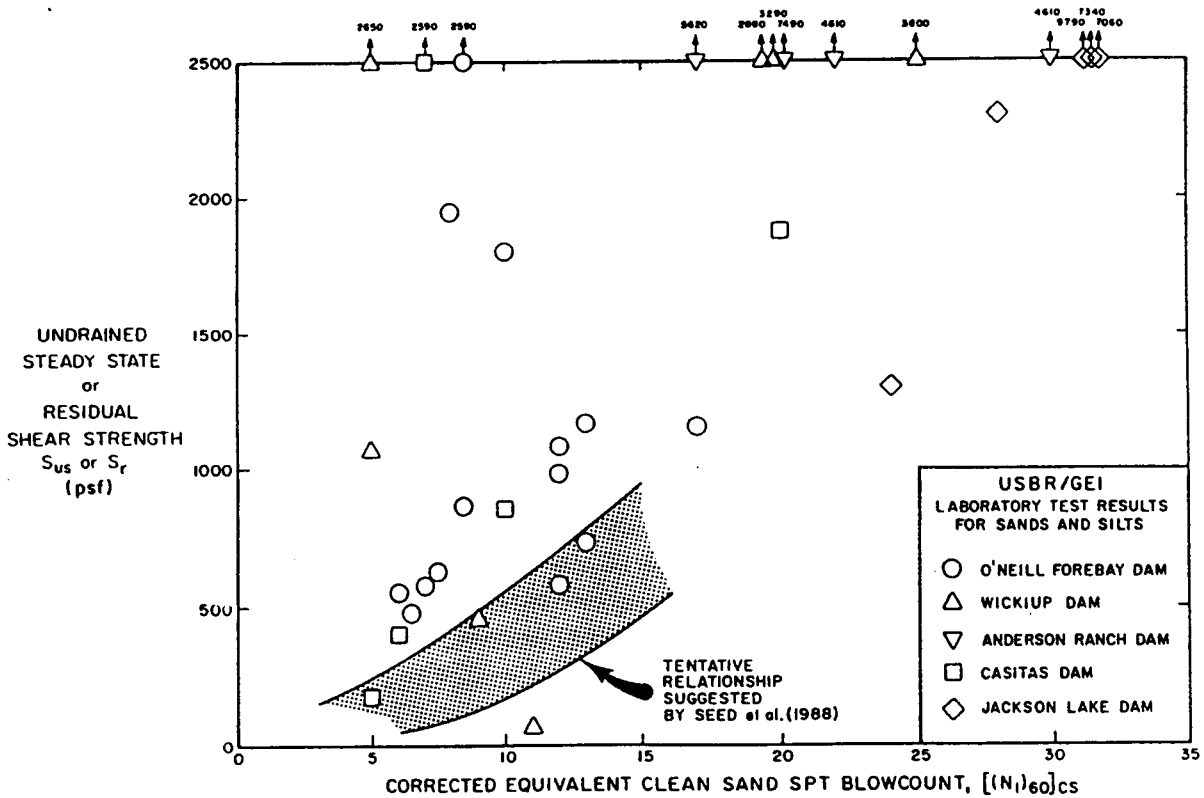


Figure 2: Comparison of Estimates of In-Situ $S_{u,r}$ Based on the "Steady State" Method vs. Range of Back-Calculated Values (Shaded Region) from Failure Case-Histories.

(Harder, 1988; modified from Von Thun, 1986)

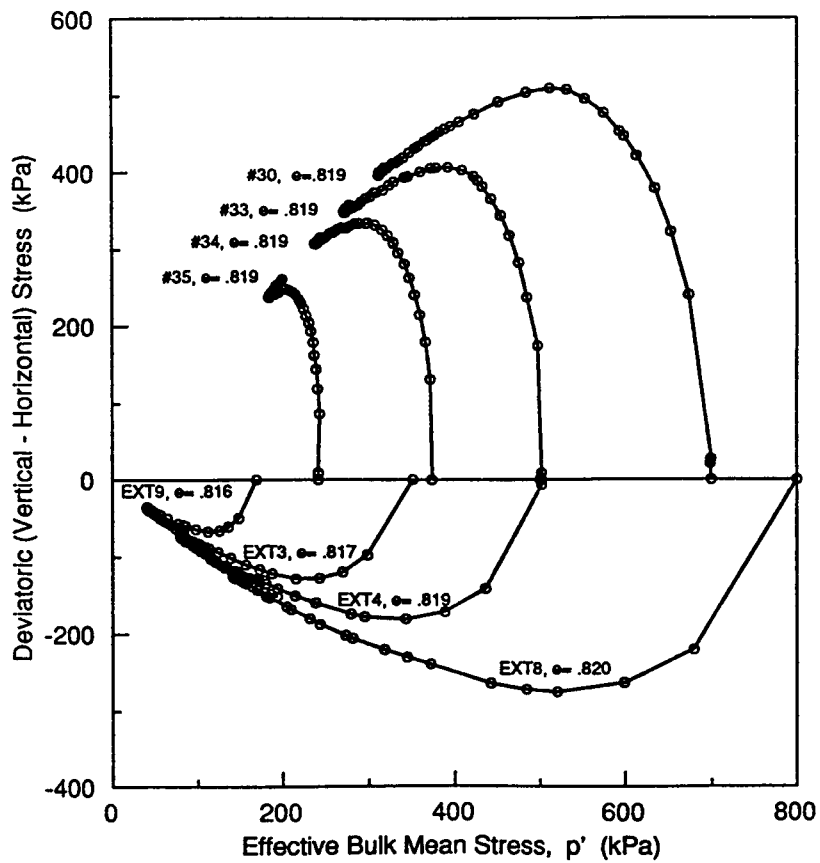


Figure 3: Stress Path Plots for Undrained Shearing of Monterey 0 Sand in Triaxial Compression (Top) and Triaxial Extension (Bottom): All Samples Consolidated to Identical Initial Void Ratio.

(Riemer, 1992)

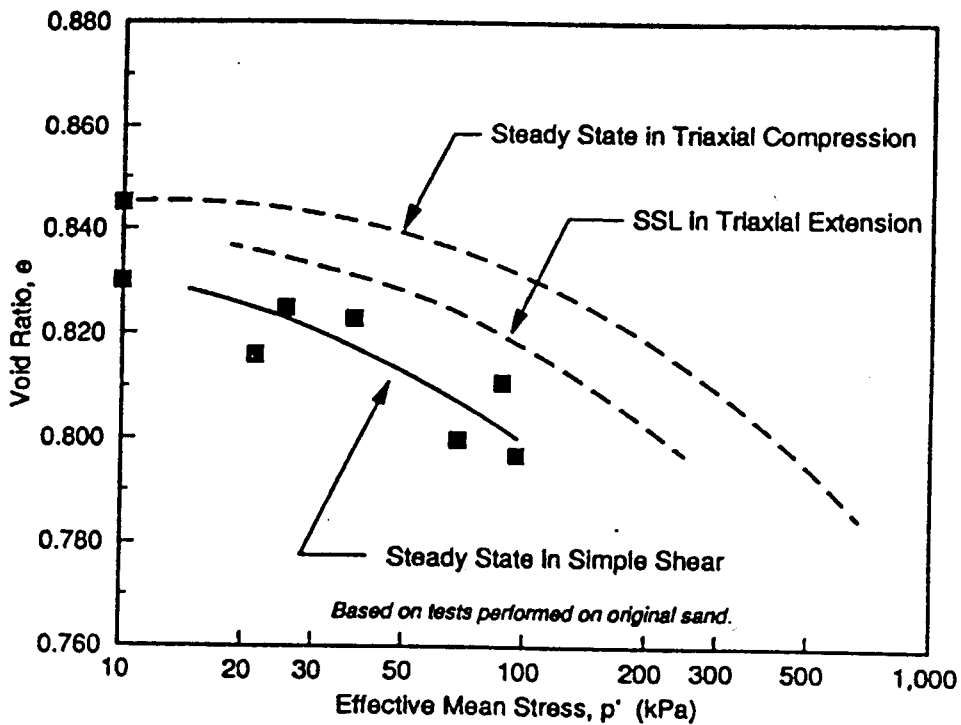
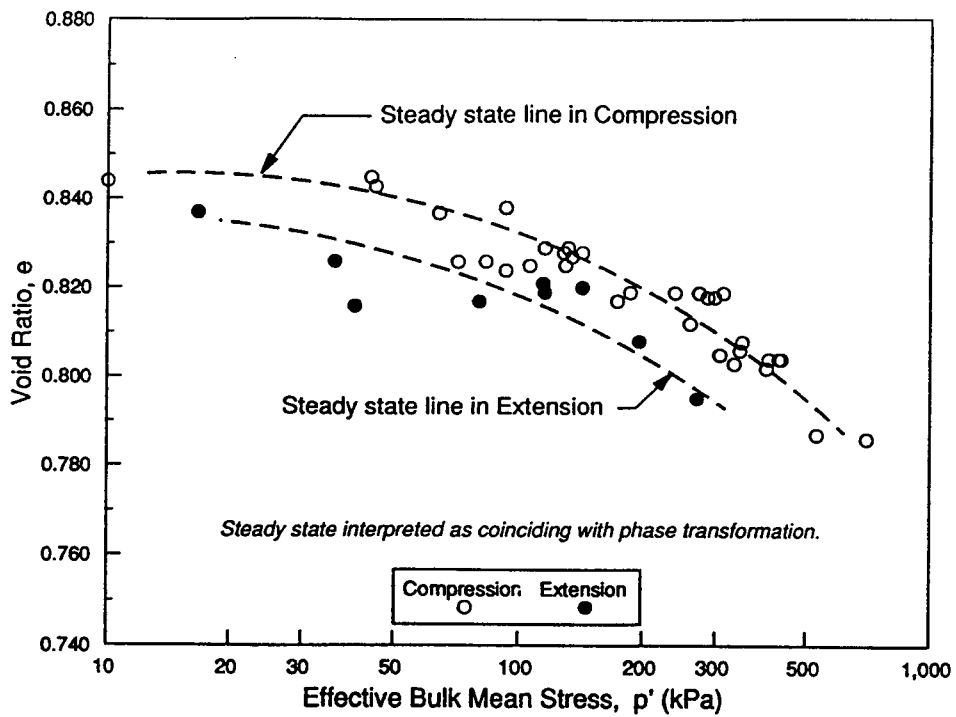


Figure 4: Steady State Lines for Monterey 0 Sand Tested in Undrained Triaxial Compression, Undrained Triaxial Extension and Undrained Simple Shear.

(Riemer, 1992)

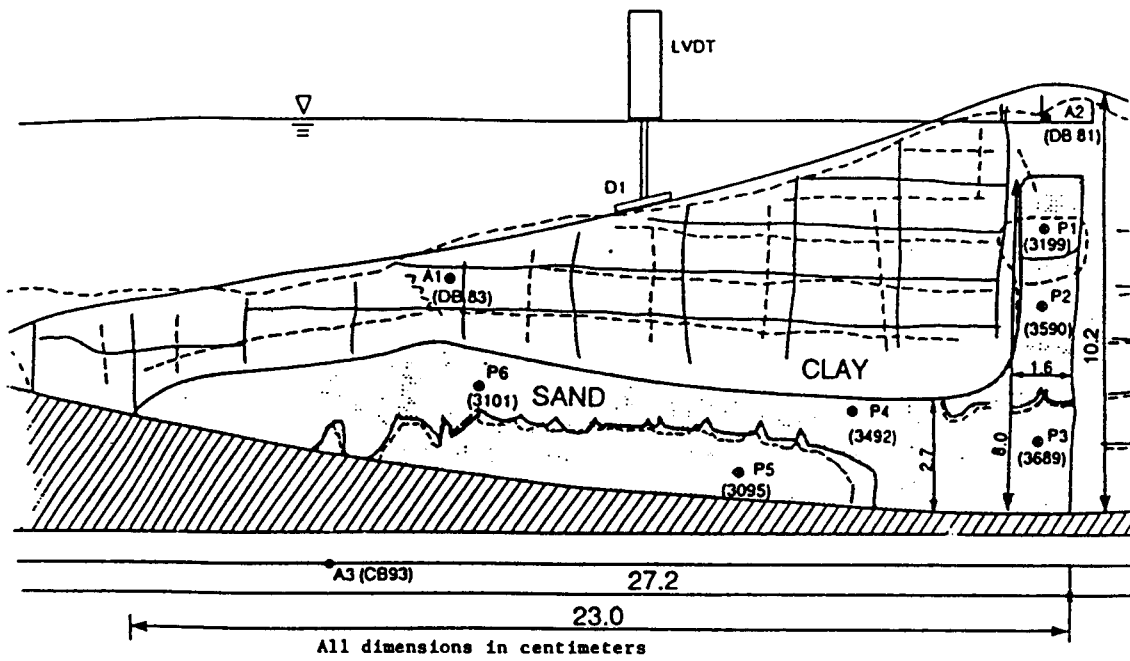


Figure 5; Centrifuge Embankment Model Illustrating Localized Void Redistribution Effects.

(Arulanandan, et al., 1993)

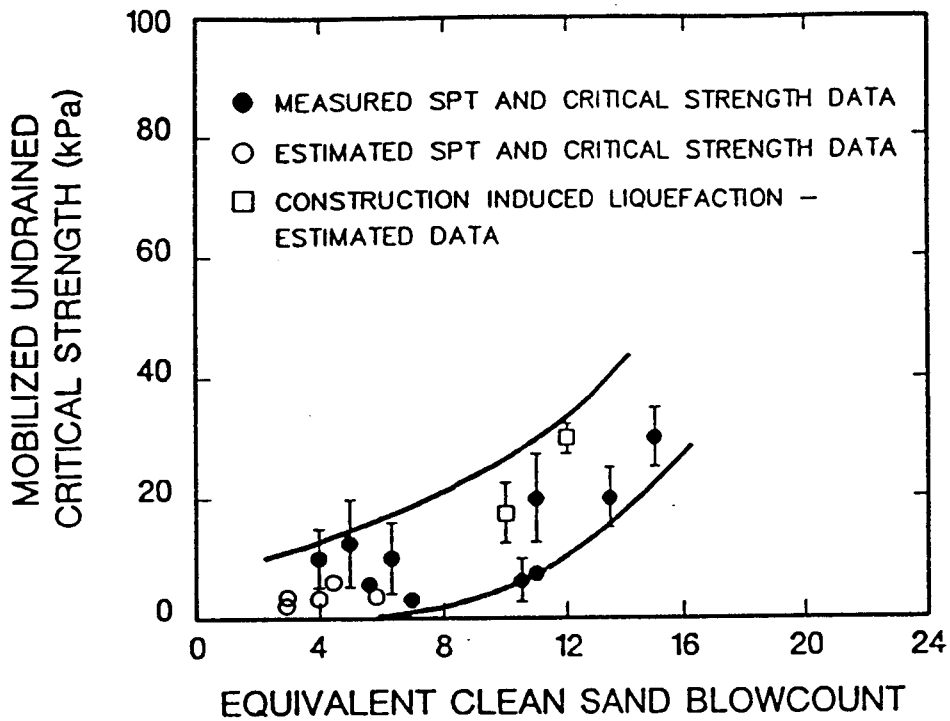


Figure 6: Recommended Correlation Between $S_{u,r}$ and $N_{1,60,cs}$
(Seed and Harder, 1990)

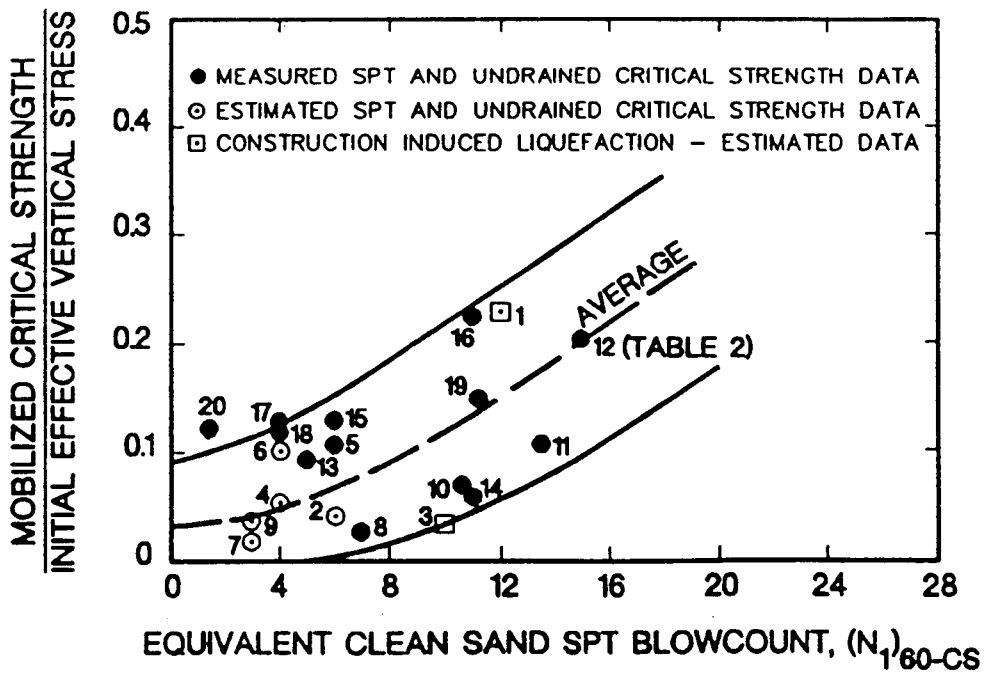


Figure 7: Back-Calculated Apparent Corellation Between $S_{u,r}/P$ and SPT Resistance
(Stark and Mesri, 1992)

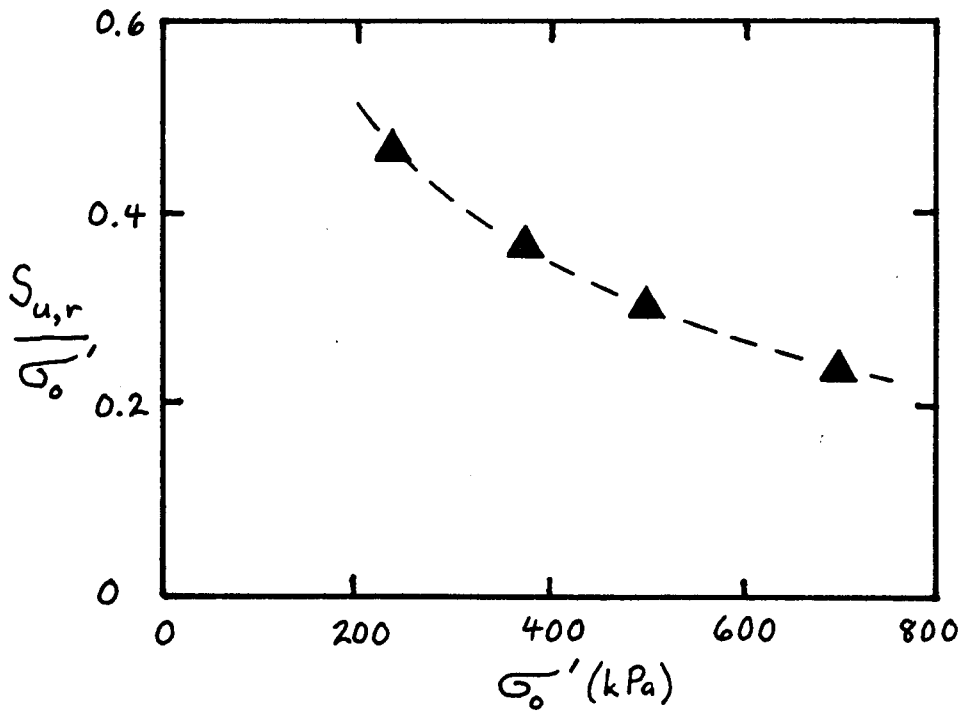
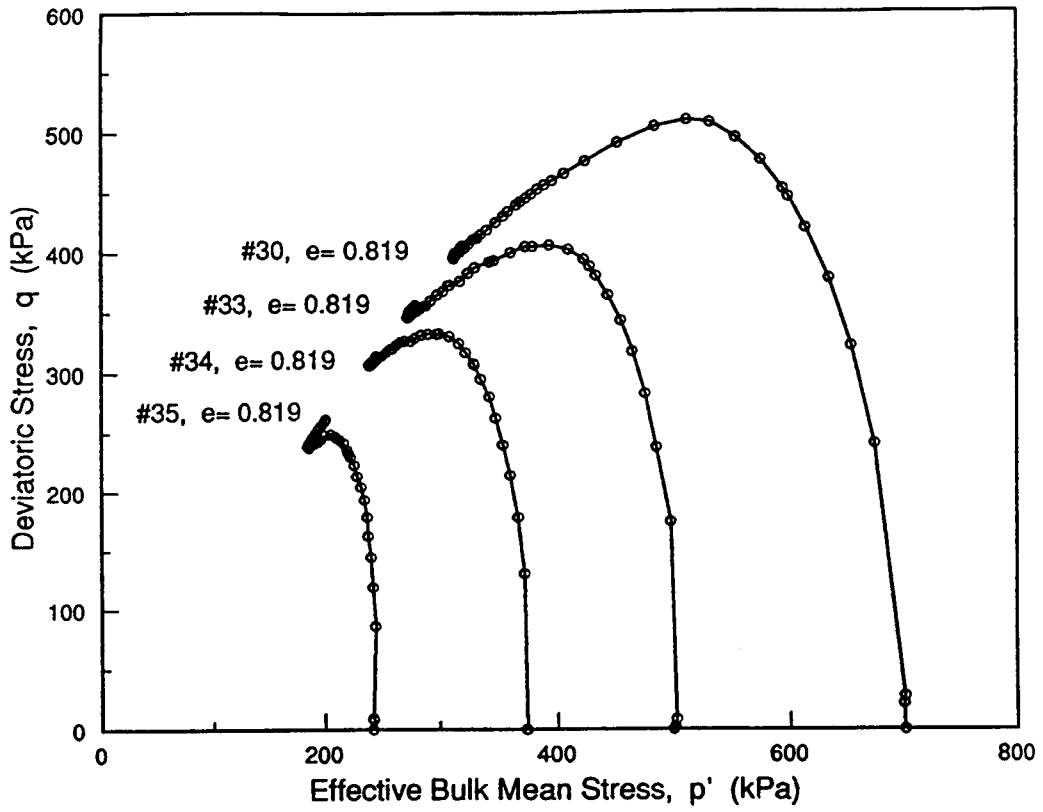


Figure 8: Illustration of Variation of $S_{u,r}/P$ as a Function of Increasing Confining Stress (P).

(Riemer, 1992)